# A New Fault Diagnosis Method Using Fault Directions in Fisher Discriminant Analysis

**Q. Peter He and S. Joe Qin**
Dept. of Chemical Engineering, The University of Texas at Austin, Austin, TX 78712

**Jin Wang**
Advanced Process Control, Advanced Micro Devices, Inc., Austin, TX 78741

*DOI 10.1002/aic.10325*
*Published online in Wiley InterScience (www.interscience.wiley.com).*

*Multivariate statistical methods such as principal component analysis (PCA) and partial least squares (PLS) have been widely applied to the statistical process monitoring (SPM) of chemical processes and their effectiveness for fault detection is well recognized. These methods make use of normal process data to define a tight normal operation region for monitoring. In practice, however, historical process data are often corrupted with faulty data. In this paper, a new process monitoring method is proposed that is composed of three parts: (1) a preanalysis step that first roughly identifies various clusters in a historical data set and then precisely isolates normal and abnormal data clusters by the k-means clustering method; (2) a fault visualization step that visualizes high-dimensional data in 2-D space by performing global Fisher discriminant analysis (FDA), and (3) a new fault diagnosis method based on fault directions in pairwise FDA. A simulation example is used to demonstrate the performance of the proposed fault diagnosis method. An industrial film process is used to illustrate a realistic scenario for data preanalysis, fault visualization, and fault diagnosis. In both examples, the contribution plots method, based on fault directions in pairwise FDA, shows superior capability for fault diagnosis to the contribution plots method based on PCA.* © 2005 American Institute of Chemical Engineers *AIChE J,* 51: 555–571, 2005

*Keywords: fault diagnosis; process monitoring; principal component analysis; contribution plot; Fisher discriminant analysis; preanalysis*

## Introduction

As chemical processes become more complex, the monitoring of chemical processes is gaining importance to assess process performance and improve process efficiency and product quality. Early detection of faults can help avoid major breakdowns and incidents. In general, four tasks are involved in the process monitoring: (1) *fault detection*, which gives an indication that something is going wrong in the process; (2) *fault identification* (or *diagnosis*), which determines the root cause of the fault; (3) *fault estimation*, which assesses the size of the fault; and (4) *fault reconstruction*, which estimates the fault-free values (Qin, 2003). Traditional fault detection and isolation (FDI) methods have been based on a mathematical model of the system. These approaches make use of the state estimation, parameter identification techniques, and parity relations to generate residuals (Benveniste, 1987; Gertler, 1988; Isermann, 1984). However, it is often difficult and time-consuming to develop accurate mathematical models that characterize all the physical and chemical phenomena occurring in industrial processes. Knowledge-based approaches such as expert systems may be considered as alternative or complementary approaches to the analytical model-based approaches

Q. P. He is also affiliated with Advanced Process Control, Advanced Micro Devices, Inc., Austin, TX 78741.
Correspondence concerning this article should be addressed to S. Joe Qin at qin@che.utexas.edu.

where analytical models are not available (Frank, 1990). However, considerable effort is also required to build these knowledge-based systems (Yoon and MacGregor, 2001).

To address the difficulties that lie in the model-based or knowledge-based methods, model-free statistical process monitoring (SPM) methods have been developed. SPM methods require only a good historical data set of normal operations, which is available for computer-controlled industrial processes. Because of the data-based nature of the SPM methods, it is relatively easy to apply to rather large and complex processes compared to model-based or knowledge-based approaches. The traditional univariate statistical process control (SPC) charts, such as the Shewhart chart, CUSUM (cumulative-sum) plot, and EWMA (exponentially weighted moving average) chart, are well-established statistical procedures for monitoring stable processes. Although univariate statistical techniques are easy to implement, they often lead to significant number of false alarms on multivariate chemical processes where the sensor measurements are highly correlated because of physical and chemical principles governing the process operation, such as mass and energy balances (Dunia and Qin, 1998). A simple yet illustrative example that shows the misleading nature of the univariate charts is given by Kourti and MacGregor (1995), where the true situation is revealed only in a multivariate plot. Multivariate statistical process control charts based on multivariate statistical methods, such as principal component analysis (PCA) and partial least squares (PLS), have been developed to overcome the shortcomings of univariate SPC.

In PCA- or PLS-based process monitoring, two indices have been widely used for fault detection: the Hotelling's $T^2$ statistic, which gives a measure of the variation with the PCA model; and the squared prediction error (SPE) of the residuals, which indicates how much each sample deviates from the model. Other less commonly used indices, such as Hawkins' $T_H^2$ (Hawkins, 1974), Mahalanobis distance, and combined indices (Raich and Cinar, 1996; Yue and Qin, 1998, 2001) have been proposed and their pros and cons are discussed in Qin (2003) and Tong and Crowe (1995).

After a fault has been detected, fault diagnosis becomes important because it is desirable to find the root cause of the fault. Currently, the well-known fault diagnosis approaches based on PCA and PLS models are the contribution plots and reconstruction-based methods (Qin, 2003). Contribution plots are very easy to generate with no prior process knowledge. Contribution plots show the contribution of each process variable to the observed statistic, that is, SPE or $T^2$. It is assumed that the process variable with high contribution is likely the root cause of the fault. However, the contribution plots may not explicitly identify the cause of an abnormal condition (Kourti and MacGregor, 1994), and sometimes may lead to incorrect conclusions. One reason is that the contribution from one variable is propagated to other variables in calculating the projection. This "smearing" effect can reduce the significance between contributing and noncontributing variables (Qin, 2003). Because of limited redundancy or correlation among the process variables, it is possible that some faults may not be identifiable (Qin, 2003).

Furthermore, the PCA approach assumes that normal data have already been isolated from historical operational data. The reality is that historical data often contain both normal and abnormal data, but little work has been done to isolate normal data from abnormal data. In this work, we start with the assumption that the historical data may contain both normal and multiple classes of abnormal data. The first step of the approach is to visualize the number of classes in the data using PCA score plots, the SPE, and $T^2$ charts. The historical data are then classified into different classes using *k*-means clustering. In the next step, we apply global Fisher discriminant analysis (FDA) to normal data and all classes of fault data to obtain a clear class visualization of high-dimensional data. In the last step, pairwise FDA is applied to normal data and each class of fault data to find fault directions that optimally separate fault data from normal data. The weights in fault directions are used to generate contribution plots for fault diagnosis. The new approach is applied to the fault diagnosis of a simulation example, the quadruple tank process, and an industrial polyester film process. The results show that the pairwise FDA provides an optimal set of fault directions in terms of distinguishing fault data from normal data and is shown to be superior for fault diagnosis compared to PCA-based contribution plots. Furthermore, in the industrial example, the visualization of lower-dimensional representation in FDA Fisher space gives a clearer view in terms of maximizing the separation among multiple classes than that in the PCA score space.

It should be noted that FDA is a widely used technique in pattern classification (Duda et al., 2001), but its use for analyzing chemical process data has not been explored until recently (Chiang et al., 2000, 2001). The basic idea of FDA is to find the Fisher optimal discriminant vector such that the Fisher criterion function is maximized. Whereas PCA seeks directions that are efficient for representation, FDA seeks directions that are efficient for discrimination. Therefore, FDA has advantages for fault visualization and diagnosis from a theoretical perspective (Chiang et al., 2000). In this work, we develop a novel fault diagnosis approach based on fault directions in pairwise FDA. Because FDA takes both normal and fault data into account and finds the fault direction that optimally separates fault data from normal data, it will be shown herein that FDA projection can reduce the effect of contribution propagation compared with PCA projection. It should be noted that neither PCA nor FDA can prevent fault propagation arising from process dynamics and/or closed-loop control. Like the contribution plot method based on PCA, the proposed method identifies the major contributing variable(s) to the fault; by this method alone, it does not identify whether the fault is the result of a sensor fault or a process fault that affects only one variable.

The organization of the paper is as follows. Section 2 gives preliminaries that provide some background knowledge on PCA, FDA, and *k*-means clustering. Section 3 introduces the new fault diagnosis method that includes data preanalysis, fault visualization, and fault diagnosis using fault directions defined by pairwise FDA. A simulation example is given in Section 4 to demonstrate the advantage of the pairwise FDA for fault diagnosis. Section 5 presents an application of preanalysis, fault visualization, and fault diagnosis to an industrial example. Conclusions based on results of this study constitute Section 6.

## Preliminary

In this section, we briefly review some relevant methods for fault diagnosis and classification. The fault detection and diagnosis method based on PCA will be introduced first, then we

will review FDA, which is the basis of the proposed fault diagnosis method. Finally, we will introduce the *k*-means clustering method, which is used in the data preanalysis.

### *PCA-based process monitoring*

Principal component analysis in many ways forms the basis of multivariate data analysis (Wold et al., 1987). Let $X^0 \in \Re^{n\times m}$ denote the raw data matrix with $n$ samples (rows) and $m$ variables (columns). $X^0$ is first scaled to a matrix $X$ with zero mean for covariance-based PCA and with unit variance for correlation-based PCA. By either the NIPALS (Wold et al., 1987) or a singular value decomposition (SVD) algorithm, the scaled matrix $X$ is decomposed as follows

$$X = TP^T + \tilde{X} = TP^T + \tilde{T}\tilde{P}^T = [T\tilde{T}][P\tilde{P}]^T \tag{1}$$

where $T \in \Re^{n\times l}$ and $P \in \Re^{m\times l}$ are the score matrix and the loading matrix, respectively. The PCA projection reduces the original set of $m$ variables to $l$ principal components. The decomposition is made such that $[T\tilde{T}]$ is orthogonal and $[P\tilde{P}]$ is orthonormal. The columns of $P$ are actually eigenvectors of the covariance or correlation matrix of the variables associated with the $l$ largest eigenvalues, and the columns of $\tilde{P}$ are the remaining eigenvectors. For fault detection in a new sample vector $x$, the squared prediction error (SPE) and Hotelling's $T^2$ are often used. The SPE statistic indicates how well each sample conforms to the model, measured by the projection of the sample vector on the residual space

$$SPE = \Box\tilde{x}\Box^2 = \Box(I - PP^T)x\Box^2 \tag{2}$$

The process is considered normal if

$$SPE \leq \delta_\alpha^2 \tag{3}$$

where $\delta_\alpha^2$ denotes the upper control limit for SPE with a significance level $\alpha$. An expression for $\delta_\alpha^2$ has been developed by Jackson and Mudholkar (1979), assuming that $x$ follows a normal distribution.

Hotelling's $T^2$ is a measure of the variation in principal component space

$$T^2 = x^T P \Lambda^{-1} P^T x \tag{4}$$

The $T^2$ statistic forms an ellipse, which represents the joint limits of variations that can be explained by a set of common causes. For a given significance level $\alpha$, the process is considered normal if

$$T^2 \leq T_\alpha^2 \tag{5}$$

where the upper control limit $T_\alpha^2$ can be calculated or approximated in several ways (Qin, 2003). If both process data $X$ and quality data $Y$ are available and one wishes to extract variations in $X$ that contribute to $Y$, PLS should be used instead of PCA. PLS attempts to extract the latent variables that not only explain the variations in the process data $X$, but also the variations in $X$ that are more predictive of the quality data $Y$. Because only the process data will be used in this work, PLS will not be discussed. Interested readers should refer to Kourti and MacGregor (1995), Kresta et al. (1991), and Wise and Gallagher (1996).

The SPE and Hotelling's $T^2$ are adequate to detect when the process is out of control, but they cannot indicate which variables are responsible for the malfunction. The contribution plots are well-known tools for fault diagnosis (Kourti and MacGregor, 1994, 1996; MacGregor, 1994; MacGregor et al., 1994; Miller et al., 1998), which break down the SPE or $T^2$ into each element corresponding to the contribution from each variable. The contribution for SPE is simply breaking down the SPE into each element

$$SPE = \sum_{i=1}^{m} \tilde{x}_i^2 \tag{6}$$

where $\tilde{x}_i$ is the contribution to SPE from the $i$th variable. If a sample has an abnormal SPE, the variables with the largest contributions are investigated.

The contribution plot on PCA scores indicates how significant the effect of each variable on the $T^2$ is. The variables with the largest contributions are considered major contributors to the fault. The $T^2$ contribution can be defined in several ways (Miller et al., 1998; Nomikos, 1997; Qin et al., 2001; Westerhuis et al., 2000). Upper control limits for contribution plots are discussed in Conlin et al. (2000), Qin et al. (2001), and Westerhuis et al. (2000).

### *Fisher discriminant analysis*

Fisher discriminant analysis is a widely used technique in pattern classification. The basic idea of FDA is to find the Fisher optimal discriminant vector such that the Fisher criterion function is maximized. The higher-dimensional feature space then can be projected onto the obtained optimal discriminant vectors for constructing a lower-dimensional feature space. Let $X \in \Re^{n\times m}$ be a set of $m$-dimensional samples $x \in \Re^m$ and the matrix $X_i$ is the subset containing $n_i$ rows of $X$ corresponding to the samples from class $i$. If $\bar{x}_i$ is the $m$-dimensional sample mean for class $i$ given by

$$\bar{x}_i = \frac{1}{n_i} \sum_{x\in X_i} x \tag{7}$$

then the within-class scatter matrix is given by

$$S_w = \sum_{i=1}^{c} P(\omega_i) S_i \tag{8}$$

where

$$S_i = \frac{1}{n_i} \sum_{x\in X_i} (x - \bar{x}_i)(x - \bar{x}_i)^T \tag{9}$$

is the within-class scatter matrix for class $i$ and $P(\omega_i)$ is the a priori probability of class $i$, generally, $P(\omega_i) = 1/c$.

Let $\bar{x}$ be the mean vector of all samples in $X$; the between-class scatter matrix is then defined by

$$S_b = \sum_{i=1}^{c} P(\omega_i)(\bar{x}_i - \bar{x})(\bar{x}_i - \bar{x})^T \tag{10}$$

The optimal discriminant direction is found by maximizing the Fisher criterion

$$J(\varphi) = \frac{\varphi^T S_b \varphi}{\varphi^T S_w \varphi} \tag{11}$$

where the maximizer $\varphi$ is the Fisher optimal discriminant direction that maximizes the ratio of the between-class scatter to the within-class scatter. It is easy to show that a vector $\varphi$ that maximize $J(\cdot)$ must satisfy

$$S_b \varphi = \lambda S_w \varphi \tag{12}$$

for some constant $\lambda$, which is a generalized eigenvalue problem. If $S_w$ is nonsingular, we can obtain a conventional eigenvalue problem by the following expression

$$S_w^{-1} S_b \varphi = \lambda \varphi \tag{13}$$

### *k-means clustering*

Industrial data usually contain both normal and abnormal data in high-dimensional space, making it difficult to segregate manually. In this work, *k*-means clustering is used to isolate different classes of data. *k*-means clustering can best be described as a partitioning method that partitions the samples in the data set into mutually exclusive clusters. Unlike the hierarchical clustering methods, *k*-means clustering does not create a tree structure to describe the groupings in the data set, but rather creates a single level of clusters. Compared to hierarchical clustering methods, *k*-means is more effective for clustering large amounts of data. The number of clusters $k$ needs to be determined at the onset. The idea behind *k*-means clustering is to divide the samples into $k$ clusters such that some metric relative to the centroids of the clusters is minimized. Various metrics to the centroids that can be minimized include:

- maximum distance to its centroid for any sample
- sum of the average distance to the centroids over all clusters
- sum of the variance over all clusters
- total distance between all samples and their centroids

The metric to minimize and the choice of a distance measure will determine the shape of the optimum clusters.

Suppose we are given $X \in \Re^{m \times n}$, a set of $m$ samples in $n$-dimensional space $\Re^n$, and an integer $k$, and the problem is to determine a set of $k$ centroids $\mu_1, \mu_2, \ldots, \mu_k$ in $\Re^n$, so as to minimize the sum-of-squares criterion

$$J = \sum_{c=1}^{k} \sum_{j=1}^{n} \| x_j - \mu_c \|^2 \tag{14}$$

A general algorithm is:

1. Randomly pick $k$ samples in the data set as the initial cluster centroids $\mu_1^{(0)}, \mu_2^{(0)}, \ldots, \mu_k^{(0)}$. Set iteration $i = 0$.
2. Assign each sample $x_j$ to the cluster with the nearest centroid $\mu_c^{(i)}$.
3. When all samples have been assigned, recalculate the positions of the $k$ centroids, as follows
$$\mu_c^{(i+1)} = E\{x_j\}_{x_j \in \mu_c^{(i)}} \tag{15}$$
4. Repeat Steps 2 and 3 until the centroids no longer move.

The above *k*-means algorithm uses an iterative procedure that converges to one of the local minima. The computational complexity is $O(mnkT)$, where $T$ is the number of iterations. In practice, the number of iterations is generally much less than the number of samples (Duda et al., 2001). It is known that *k*-means are sensitive to initial starting conditions. Despite this limitation, the algorithm is used fairly frequently as a result of its ease of implementation. One way to determine good optima is to do many runs of *k*-means, each from a different random starting point, and select the best minimum in terms of Eq. 14.

In practice, a few issues need to be addressed when using *k*-means clustering. The number of clusters $k$ is determined by incorporating information from process knowledge, visualizing clusters in the original or transformed variable space with a preliminary PCA, and other knowledge that can enhance the accuracy of the clustering. If more than one possible $k$ exist (that is, the normal data and the abnormal data do not have clear-cut clustering sets), it is practical to try different clustering arrangements to obtain the best result for different monitoring purposes. If normal data have different clustering sets arising from differences in operational conditions, *k*-means clustering should be used in a supervised manner, that is, those clusters with known class labels should be bonded to those class labels either by fixing their class identity or using weightings to guarantee correct classification.

### *Fault Diagnosis Using Fault Directions in FDA*

In this section, we present our proposed approach in three steps: data preanalysis, fault visualization, and fault diagnosis. We start with the assumption that the historical data contain unclassified normal and multiple classes of abnormal data. By incorporating process knowledge, the first step of the approach is to visualize the number of classes in the data using PCA score plots, SPE chart, and $T^2$ chart; the historical data are then classified into different classes using *k*-means clustering. In the next step, global FDA is applied to obtain a clear fault visualization in 2-D or 3-D Fisher space. Finally, pairwise FDA is applied to normal data and each class of fault data to find fault direction that optimally separates each fault data from normal data. The weights in fault directions are used to generate contribution plots for fault diagnosis. The entire process, including preanalysis of historical data, fault visualization, and fault diagnosis, is summarized in Figure 1 and each step is discussed in the following subsections.

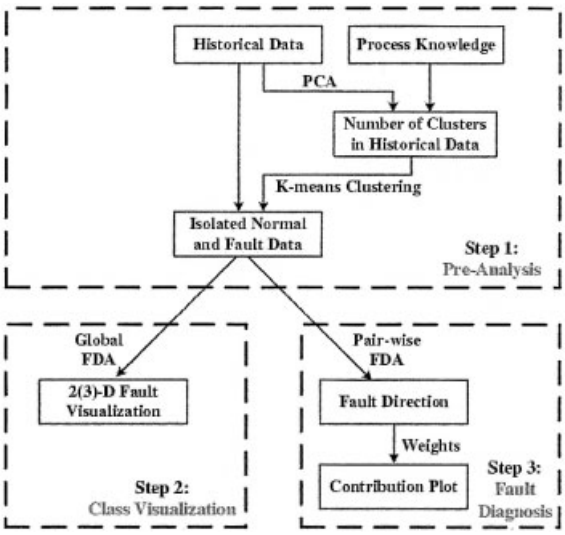


**Figure 1. Overall flowchart of the proposed preanalysis, fault visualization, and fault diagnosis method.**

### *Data preanalysis*

In this step, a PCA model is built for the whole data set, which contains both normal and abnormal data. Clusters are visualized in PCA 2-D or 3-D score space. The total number of clusters $k$ can usually be revealed in the PCA score plot, although the clusters are not maximally separated. Then a finer analysis that incorporates process knowledge is conducted to determine the total number of clusters $k$ in the data. The objective is to identify enough normal samples to build the normal PCA model. Ambiguous data points during the transition between clusters can be ignored. After $k$ is identified, $X$ is partitioned into $k$ disjoint classes: $X_0, X_1, \ldots, X_{k-1}$ by applying $k$-means clustering. This step usually involves several iterations by incorporating process knowledge.

### *Fault visualization*

Data visualization is an active research field in computer science and is a desirable feature for process engineers to perform fault diagnosis. Although the data are high dimensional, it is possible to project the fault classes to low-dimensional space using dimension-reduction techniques such as PCA and FDA.

In this step, we apply global FDA to all classes identified in the first step. The within-class and between-class scatter matrices are calculated by Eqs. 8 and 10. Similar to the score plot based on PCA, we project high-dimensional data onto $\varphi_1$ and $\varphi_2$, corresponding to the first two largest eigenvalues $\lambda_1$ and $\lambda_2$, to obtain 2-D visualization of normal and fault data in FDA Fisher space. Because of the discrimination nature of FDA, we will have a better fault visualization than that in the PCA score space. This will be demonstrated in an industrial example in a subsequent section.

### *Fault diagnosis*

After the normal and fault data are properly classified, the next step is to characterize faults by pairwisely applying FDA to normal data, denoted as $X_0$, and each class of fault data $X_i$ ($i = 1, \ldots, k-1$). The scatter matrix for normal data $X_0$ is

$$S_0 = \frac{1}{n_0} \sum_{x \in X_0} (x - \bar{x}_0)(x - \bar{x}_0)^T \tag{16}$$

The scatter matrix for fault data $X_i$ ($i = 1, \ldots, k-1$) is

$$S_i = \frac{1}{n_i} \sum_{x \in X_i} (x - \bar{x}_i)(x - \bar{x}_i)^T \tag{17}$$

Therefore the within-class scatter matrix is

$$S_w = S_0 + S_i \tag{18}$$

Let $\bar{x}$ be the mean vector of samples in $X_0$ and $X_i$; the between-class scatter matrix is then given by

$$S_b = \sum_{j=0,i} (\bar{x}_j - \bar{x})(\bar{x}_j - \bar{x})^T \tag{19}$$

Because we include only two classes in pairwise FDA analysis, by substituting Eqs. 18 and 19 into Eq. 12 and solving the generalized eigenvalue problem we will obtain only one significant eigenvalue $\lambda_i$ and one Fisher direction, that is, the eigenvector $\varphi_i$, corresponding to this single significant $\lambda_i$. This Fisher direction is the optimal direction that discriminates fault data $X_i$ from normal data $X_0$ according to the Fisher criterion. This direction best characterizes the effect of the fault relative to the normal data. Therefore, we define this Fisher direction $\varphi_i$

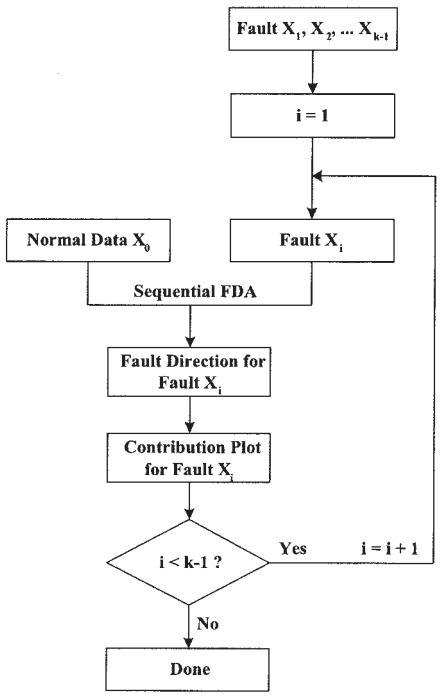


**Figure 2. Pairwise FDA flowchart.**

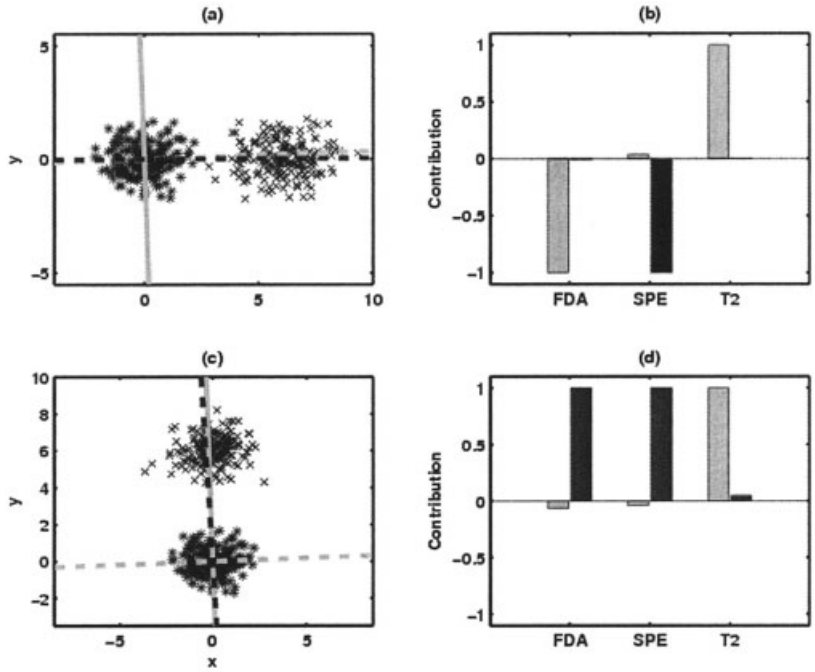


**Figure 3. (a) Scatter plot, case 1; (b) contribution plots, case 1; (c) scatter plot, case 2; (d) contribution plots, case 2.**

as the fault direction for $X_i$. The weights in $\varphi_i$ are used to generate the contribution plot for fault $X_i$. For a fault direction

$$\varphi_i = [\phi_1, \phi_2, \ldots, \phi_j, \ldots, \phi_m]^T \tag{20}$$

the $j$th element $\phi_j$ is the contribution from the $j$th variable. Note that $\phi_j$ represents an average contribution over $n_i$ samples in $X_i$ because the fault direction is calculated based on all samples in $X_i$. The new fault diagnosis method is illustrated in Figure 2, where we start with isolated normal and fault data obtained from data preanalysis. The fault direction is calculated by performing pairwise FDA on normal and each class of fault data, after which we examine the contribution plot based on the fault direction to determine the root cause of the fault. This process is repeated until all faults are analyzed. Notice that for pairwise FDA, the fault direction can be computed efficiently using the power method, given that only the eigenvector associated with the largest eigenvalue is needed.

A simple illustrative example is used here to demonstrate the procedure of finding fault directions and creating contribution plots using fault directions in pairwise FDA. The data are generated in the following way using Matlab where different seeds are used for random number generation:

*Normal Samples ($x_0$, $y_0$)*

$$x_0 = \text{randn}(200, 1)$$

$$y_0 = 0.7 * \text{randn}(200, 1)$$

*Fault Samples ($x_1$, $y_1$) with Bias in the x Direction*

$$x_1 = \text{randn}(200, 1) + 6$$

$$y_0 = 0.7 * \text{randn}(200, 1)$$

Figure 3a shows the scatter plot of the samples where stars are normal samples and $\times$ marks are fault samples with a mean shift in the $x$ direction. By performing FDA on normal and fault data, we find fault direction $\varphi_1 = [0.99998 \;\; 0.00569]^T$, which is shown in Figure 3a as black dash line. For comparison, PCA direction is shown as a gray dash line and PCA residual direction is shown as a gray solid line in the same plot. The contribution plot is shown as the bar chart of $\varphi_1$ in Figure 3b, where the gray bar is the contribution from $x$ and the black bar is the contribution from $y$. Also included in Figure 3b are averaged contributions to SPE and $T^2$ based on PCA. We observe that contribution plot based on

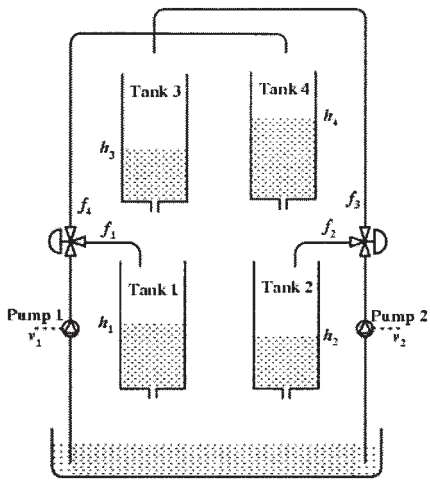


**Figure 4. Schematic diagram of the quadruple-tank process.**

**Table 1. Simulation Parameters***

| Parameter | Unit | Value |
|---|---|---|
| $A_1$; $A_3$ | $cm^2$ | 28 |
| $A_2$; $A_4$ | $cm^2$ | 32 |
| $a_1$; $a_3$ | $cm^2$ | 0.071 |
| $a_2$; $a_4$ | $cm^2$ | 0.057 |
| $k_1$; $k_2$ | $cm^3\ V^{-1}\ s^{-1}$ | 3.33 |
| $g$ | $cm/s^2$ | 981 |

*After Johannson (2000).

FDA and PCA $T^2$ correctly indicate that a fault in the $x$ direction is the root cause of the fault ,whereas the PCA SPE-based contribution plot leads to the opposite conclusion. Now we look at another situation where we have a bias fault in the $y$ direction instead of in the $x$ direction:

Fault samples ($x_2$, $y_2$) with a bias in the $y$ direction are generated as follows

$$x_2 = \text{randn}(200, 1)$$

$$y_2 = 0.7 * \text{randn}(200, 1) + 6$$

The scatter plot is shown in Figure 3c. It can be seen in Figure 3d that the contribution plot based on PCA $T^2$ gives an incorrect conclusion, whereas contribution plots based on PCA SPE give correct fault direction, which is similar to the fault direction in FDA.

To summarize, contribution plots based on PCA $T^2$ and SPE do not give consistent conclusions for these two cases, whereas contribution plots based on FDA fault directions give correct and consistent conclusions. Here we did not scale the variance of the data. If the normal data were scaled to unit variance, the fault direction angle based on PCA would be 45° and the contributions would be the same for the two variables, irrespective of what kind of fault occurred to the fault data (Qin, 2003).

In the next two sections, the new approach is applied to the fault diagnosis of a simulation example, quadruple-tank process, and an industrial polyester film process.

## Simulation Example

In this section, the quadruple-tank process is used as a simulation example to demonstrate the advantage of the pairwise FDA for fault diagnosis. The quadruple-tank process was originally developed by Johansson (2000) as a novel multivariate laboratory process. This process consists of four interconnected water tanks, two pumps, and associated valves. A schematic diagram of the process is shown in Figure 4. The inputs are the voltages supplied to the pumps, $v_1$ and $v_2$, and the outputs are the water levels $h_1$–$h_4$. The flow to each tank is adjusted using the associated valves $\gamma_1$ and $\gamma_2$. A nonlinear model is derived based on mass balances and Bernoulli's law

$$\frac{dh_1}{dt} = -\frac{a_1}{A_1}\sqrt{2gh_1} + \frac{a_3}{A_1}\sqrt{2gh_3} + \frac{\gamma_1 k_1}{A_1} v_1 \tag{21}$$

$$\frac{dh_2}{dt} = -\frac{a_2}{A_2}\sqrt{2gh_2} + \frac{a_4}{A_2}\sqrt{2gh_4} + \frac{\gamma_2 k_2}{A_2} v_2 \tag{22}$$

$$\frac{dh_3}{dt} = -\frac{a_3}{A_3}\sqrt{2gh_3} + \frac{(1-\gamma_2)k_2}{A_3} v_2 \tag{23}$$

$$\frac{dh_4}{dt} = -\frac{a_4}{A_4}\sqrt{2gh_4} + \frac{(1-\gamma_1)k_1}{A_4} v_1 \tag{24}$$

For tank $i$, $A_i$ is the cross section of the tank, $a_i$ is the cross section of the outlet hole, and $h_i$ is the water level. The voltage

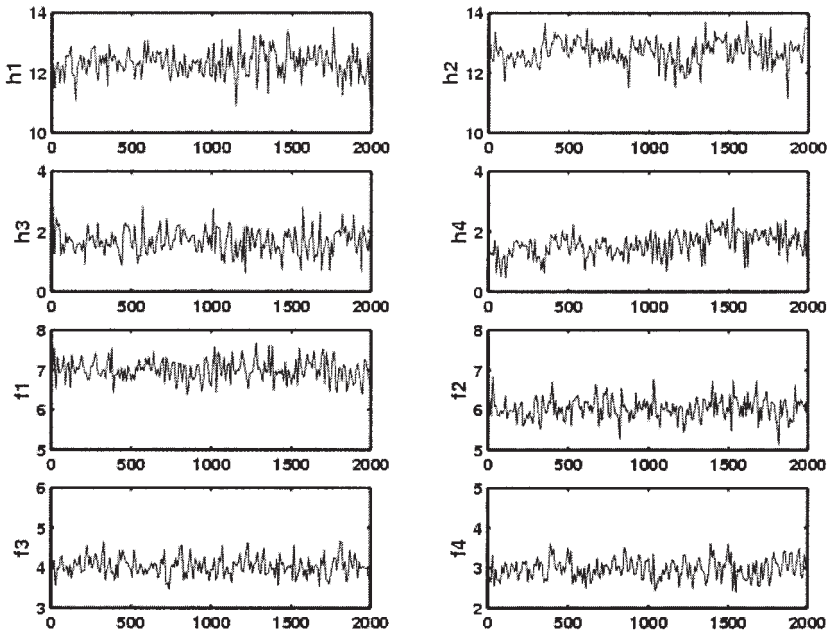


**Figure 5. Process time series data with sensor fault in $h_4$.**

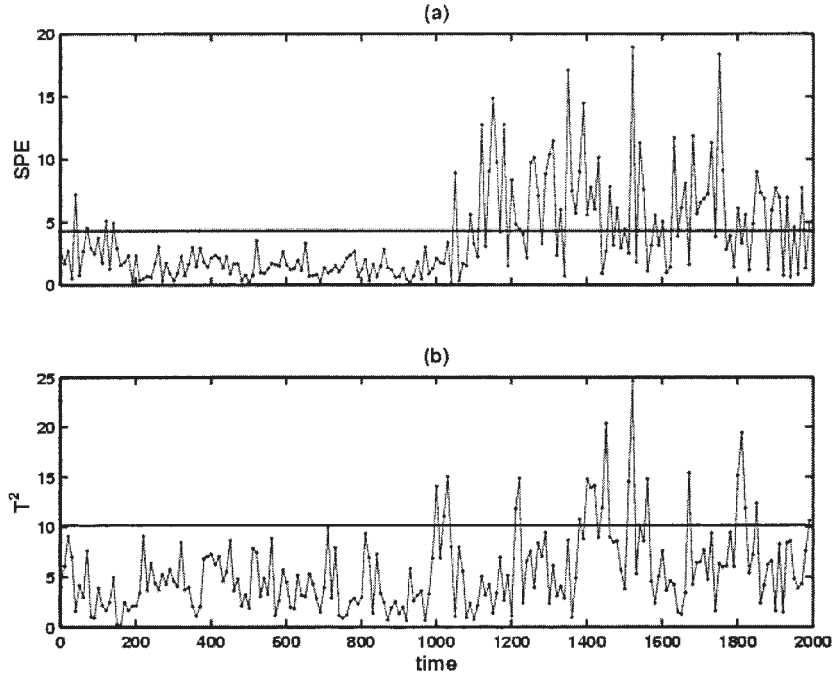


**Figure 6. SPE and $T^2$ charts with 95% limit (the sensor fault in $h_4$ is introduced after 1000 s).**

applied to pump $i$ is $v_i$ and the corresponding flow is $k_i v_i$. The parameters $\gamma_1, \gamma_2 \in (0, 1)$ are determined from how the valves are set before an experiment. The water flow rate to tank 1 (that is, $f_1$) is $\gamma_1 k_1 v_1$ and the flow rate to tank 4 (that is, $f_4$) is $(1 - \gamma_1)k_1 v_1$ and similarly for tanks 2 and 3. The acceleration of gravity is denoted as $g$. The parameter values of this process are given in Table 1. The data are generated by Eqs. 21–24, where $\gamma_i$ and $v_i$ are corrupted by independently Gaussian white noise with zero mean and standard deviation of 0.01 and 0.05. respectively, which are about 1–2% of their upper limit or steady-state value. Measured $h_i$ is corrupted by Gaussian distributed white noise with zero mean and standard deviation of 0.1 and measured $\gamma_i$ and $v_i$ contain the same level of noise as the input $\gamma_i$ and $v_i$, respectively.

Two cases, sensor fault and tank leakage, are studied in this work. In both cases, PCA $T^2$ chart and SPE chart are applied to

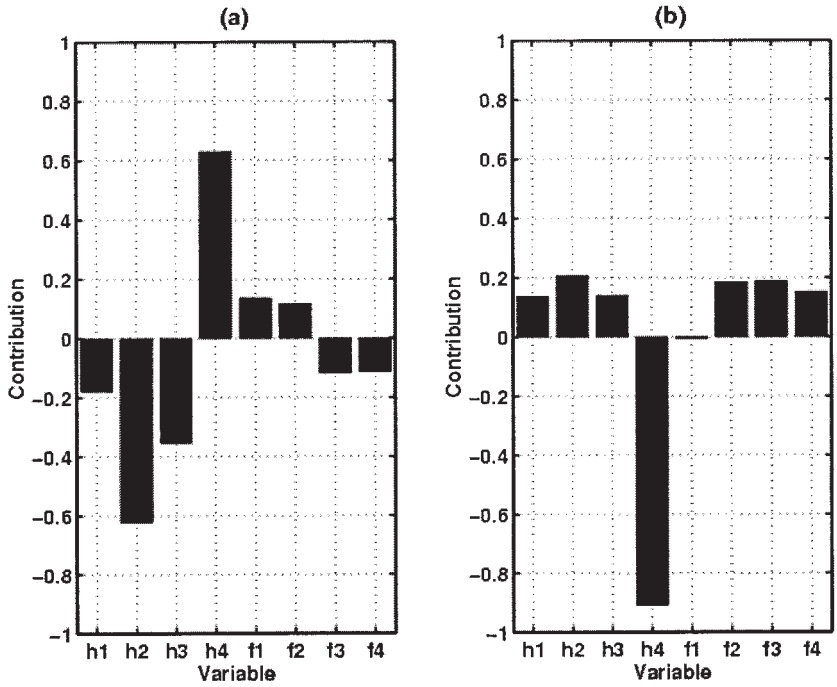


**Figure 7. Contribution plots based on PCA model (a) and FDA fault direction (b) with sensor fault in $h_4$.**

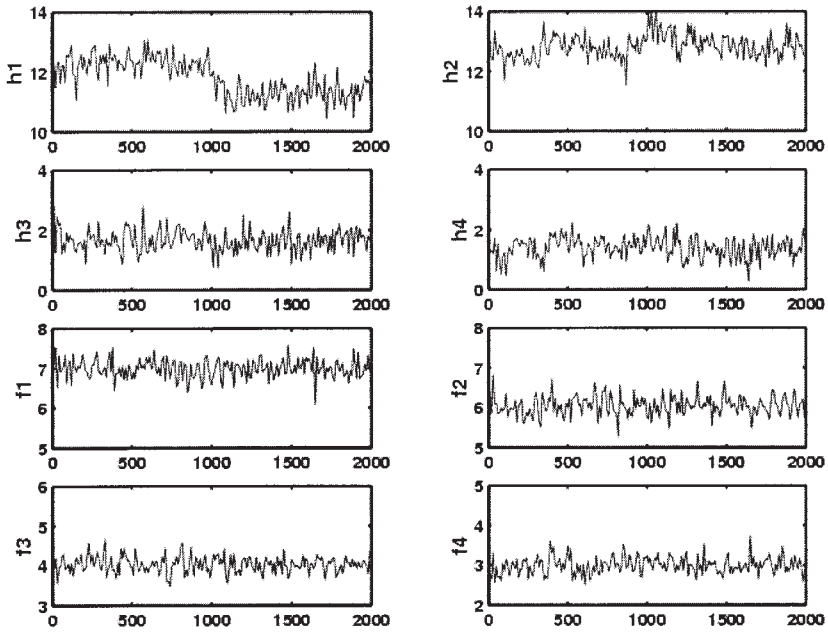


**Figure 8. Process time series data with leakage in $h_1$.**

detect the fault. Contribution plots based on both PCA and FDA fault directions are used to diagnose the fault and their performances are compared.

### *Case 1: sensor fault*

We generated 100 normal data samples using a 10-s sampling interval, and then generated an additional 100 samples with a bias fault $\Delta h_4 = 0.3$ in sensor $h_4$. Figure 5 shows the time series data of the process variables: water levels $h_1$–$h_4$ and flow rates to tanks $f_1$–$f_4$. It is almost impossible for the naked eye to detect the sensor fault in $h_4$ from these plots because of the small magnitude of the bias. First, PCA is applied to analyze these data. A PCA model is built based on the first 100 observations and 4 PCs are kept in the model, which capture about 76% of the total variance. The SPE and $T^2$ charts for normal and fault observations are given in Figure 6 with upper control limits. Both charts captured the subtle change in the process and clearly indicate that something went wrong after

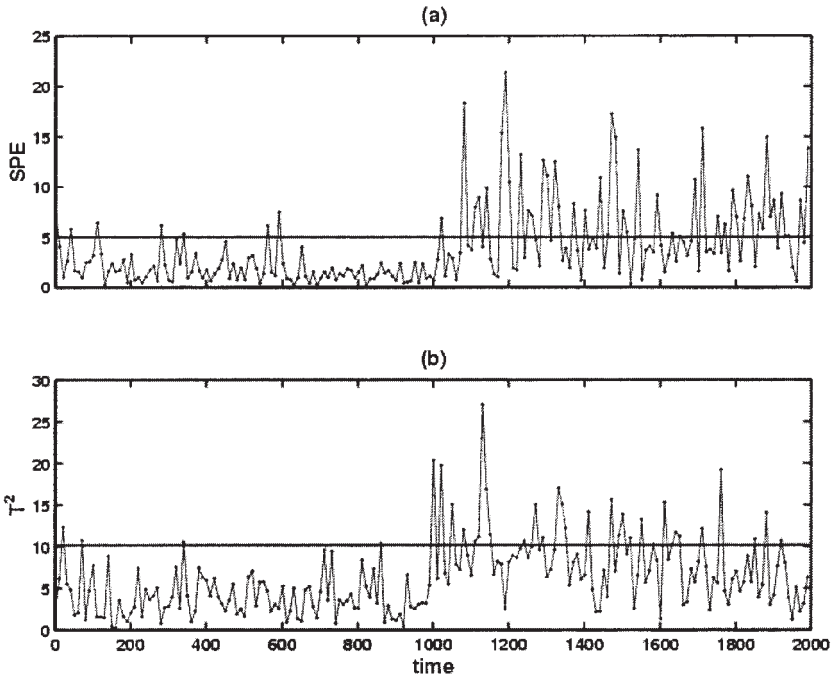


**Figure 9. SPE and $T^2$ charts with 95% limit (the leakage in $h_1$ is introduced after 1000 s).**

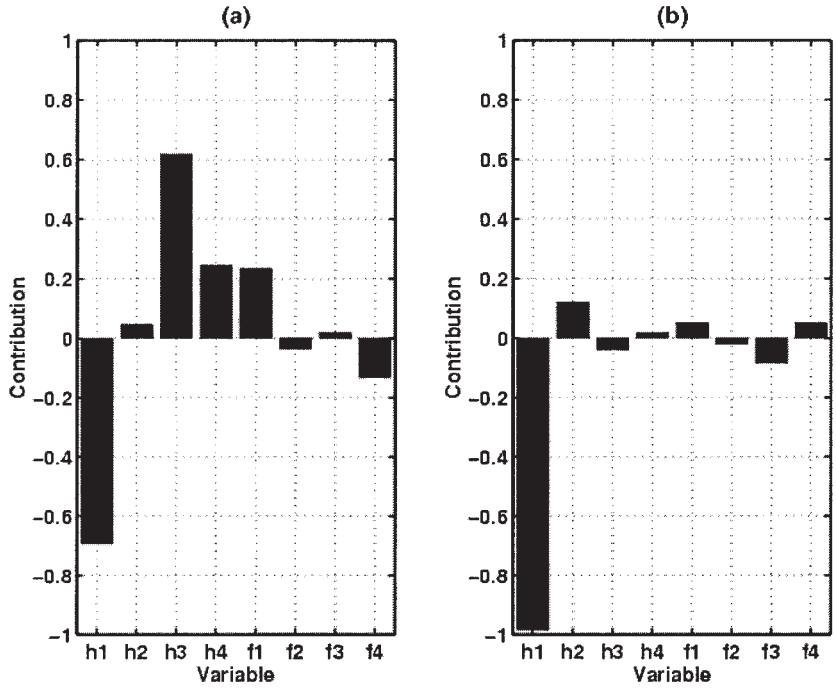


**Figure 10. Contribution plots based on PCA model (a) and FDA fault direction (b) with leakage in $h_1$.**

1000 s. A contribution plot is then created to diagnose the fault. The averaged contribution plot based on PCA SPE in Figure 7a does not explicitly indicate that $h_4$ is the root cause of the fault. Instead, both $h_2$ and $h_4$ are identified as the biggest contributors to this fault. FDA is then applied to diagnose the same fault. The FDA model is built based on the fault detection knowledge from PCA that there are two different classes of observations: the first 100 normal observations and the second 100 fault observations. The fault direction $\varphi$ is found by solving Eq. 12. The contribution plot based on FDA fault direction is shown in Figure 7b, which clearly indicates that $h_4$ is the only root cause of the fault.

### *Case 2: tank leakage*

The data generation in case 2 is similar to that in case 1. A leakage in tank 1 is introduced after 1000 s. We assume that there is a small hole at the bottom of tank 1 with the cross section $a_{\text{leak}} = 0.005$ cm$^2$. The mass balance equation for tank 1 changes from Eq. 21 to

$$\frac{dh_1}{dt} = -\frac{a_1}{A_1}\sqrt{2gh_1} + \frac{a_3}{A_1}\sqrt{2gh_3} + \frac{\gamma_1 k_1}{A_1}v_1 - \frac{a_{leak}}{A_1}\sqrt{2gh_1} \quad (25)$$

where the last term corresponds to the leakage of tank 1. Mass balance equations for the other tanks do not change. Figure 8 shows the time series data of the process variables consist of 100 normal data and 100 abnormal data. As in case 1, a PCA model is built based on normal data using 4 PCs. Both the SPE chart and the $T^2$ chart in Figure 9 correctly detect the fault. However, $h_1$ and $h_3$ are identified as the root cause of the fault, as indicated in the contribution plot based on PCA SPE in Figure 10a. Figure 10b shows the contribution plot based on the fault direction in the FDA model, which is built based on the same procedure as in case 1. Thus $h_1$ is explicitly identified as the root cause of the fault.

## Preanalysis, Visualization, and Diagnosis for an Industrial Film Process

In the simulation example, we demonstrated only the third step of the proposed approach: fault diagnosis using fault directions in FDA. Now we apply all three steps to an industrial polyester film manufacturing process. The process data contain a total of 2879 samples, which constitute a mixture of normal and abnormal samples. Each sample consists of 103 measured process or monitoring variables belonging to seven different operation zones, as shown in Table 2, to describe a unit or a specific physical or chemical operation (Qin et al., 2001). [Interested readers who want additional information about the theoretical background and practical techniques for the control of sheet and film processes are referred to Featherstone et al. (2000).] This process is used to illustrate a realistic scenario for data preanalysis, fault visualization, and fault diagnosis. In the first step, the *k*-means clustering method is used in conjunction with a PCA-based SPE chart and $T^2$ chart to classify the historical data into normal and abnormal operating regions. In

**Table 2. Polyester Film Manufacturing Process Variables Divided into Blocks***

| | | |
|---|---|---|
| 1 | Drying zone | 1–9 |
| 2 | Extrusion zone | 10–29 |
| 3 | Melt pipes zone 1 | 30–40 |
| 4 | Melt pipes zone 2 | 41–52 |
| 5 | Die zone | 53–61 |
| 6 | Casting zone | 62–77 |
| 7 | Tenter zone | 78–103 |

*After Qin et al. (2001).

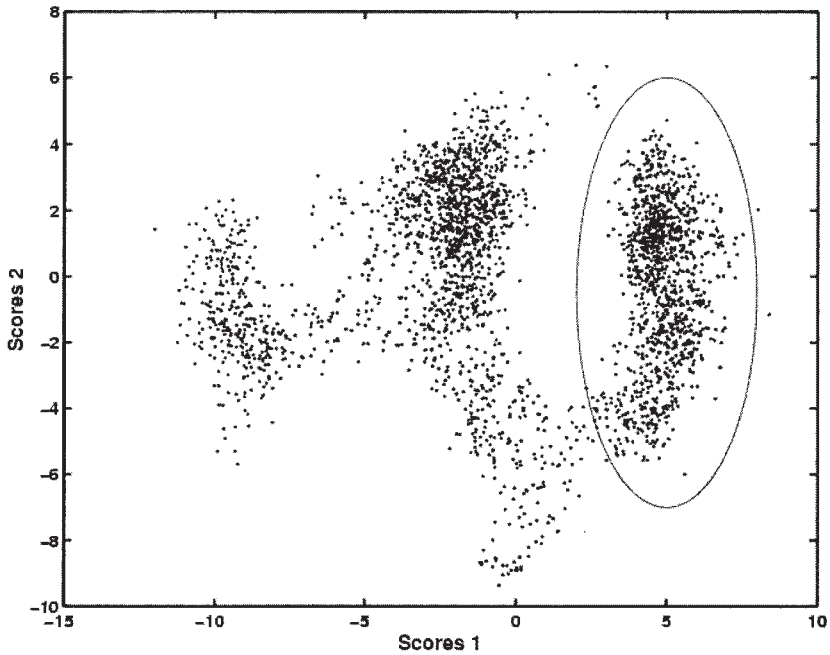


**Figure 11. Clusters in the polyester film process data.**

the second step, global FDA is applied to visualize faults in 2-D Fisher space. In the third step, pairwise FDA is applied to find fault directions that best isolate fault data from normal data. These directions are interpreted as variable contributions for fault diagnosis and their performances are compared to PCA-based contribution plots.

### *Historical data preanalysis*

A preliminary PCA score plot based on all process data is shown in Figure 11 to visualize the clusters in the data set. We can see that there are several clusters. With the help from the plant engineers we know that the data cluster with an ellipse is normal, whereas others are abnormal. From this plot it is difficult to see whether there are two or three clusters outside the ellipse. So we rebuild the PCA model based on the first 1000 normal process data only, then project the whole data set onto this PCA model. Figure 12a shows the SPE plot based on the PCA model and Figure 12b shows the Hotteling's $T^2$ plot. From these figures, we see clearly that there are four operation regions where A is the normal region, and B, C, and D are fault

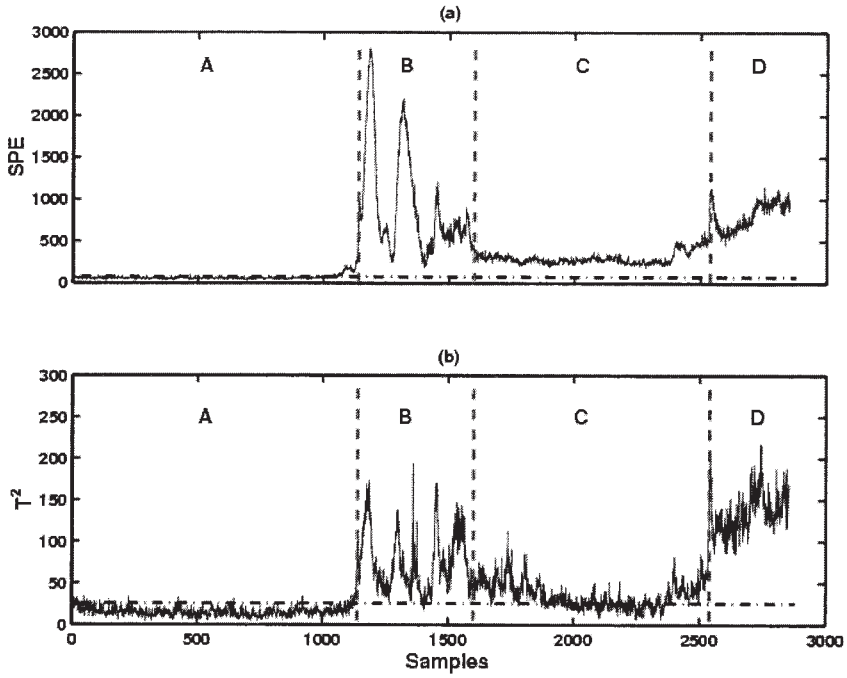


**Figure 12. (a) SPE chart and (b) $T^2$ chart.**

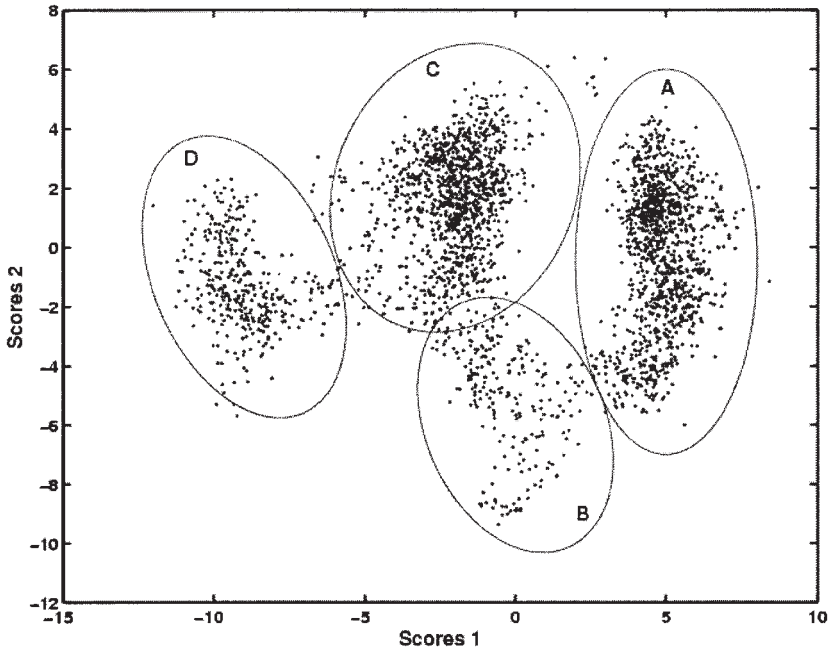


**Figure 13. PCA approximately classified clusters in PCA score space.**

regions. Figure 13 shows the PCA scores with approximately labeled regions based on SPE and $T^2$ charts in Figure 12. To determine the boundary of each region, *k*-means clustering is applied to obtain the exact category for each sample. Figure 14 shows the *k*-means clustering results in PCA scores space. The classes vs. samples are shown in Figure 15, where classes A, B, C, and D correspond to the operation regions A, B, C, and D.

### *Fault visualization*

After removing ambiguous samples from the transitional regions, we perform PCA based on all remaining samples to get an overall view of four classes, as shown in Figure 16. We also perform global FDA on this reduced data set, the results of which are shown in Figure 17. By comparing Figure 16 and Figure 17 we observe that each cluster is more compact and better separated in FDA Fisher space than in PCA score space. It is interesting to note that, in FDA Fisher space, fault C is closer to normal region A than faults B and D, which is consistent with SPE and $T^2$ plots (Figure 12) where fault C has smaller SPE and $T^2$ values than those of faults B and D, whereas we do not observe this from the PCA score plot. The comparison shows that PCA seeks directions that are efficient

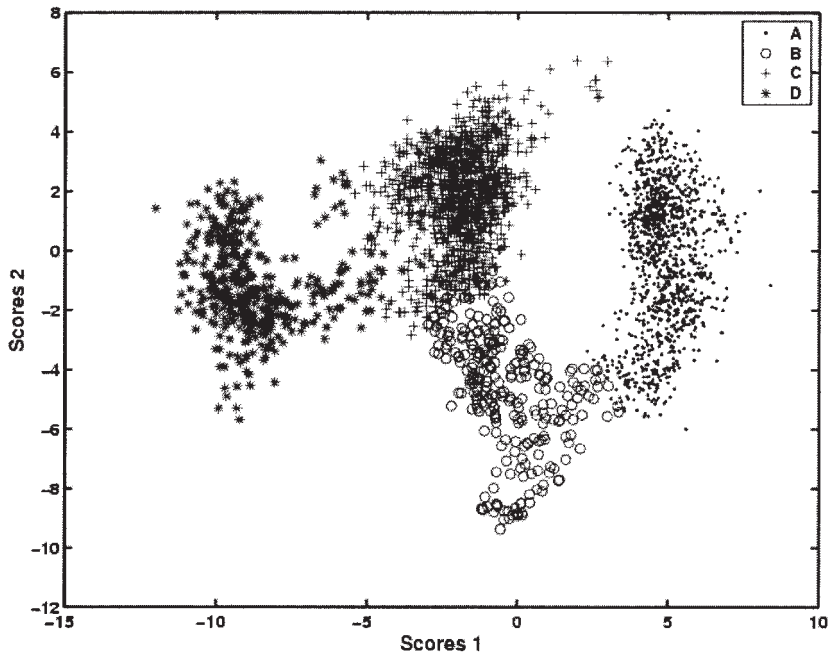


**Figure 14. *k*-means classified clusters in PCA score space.**

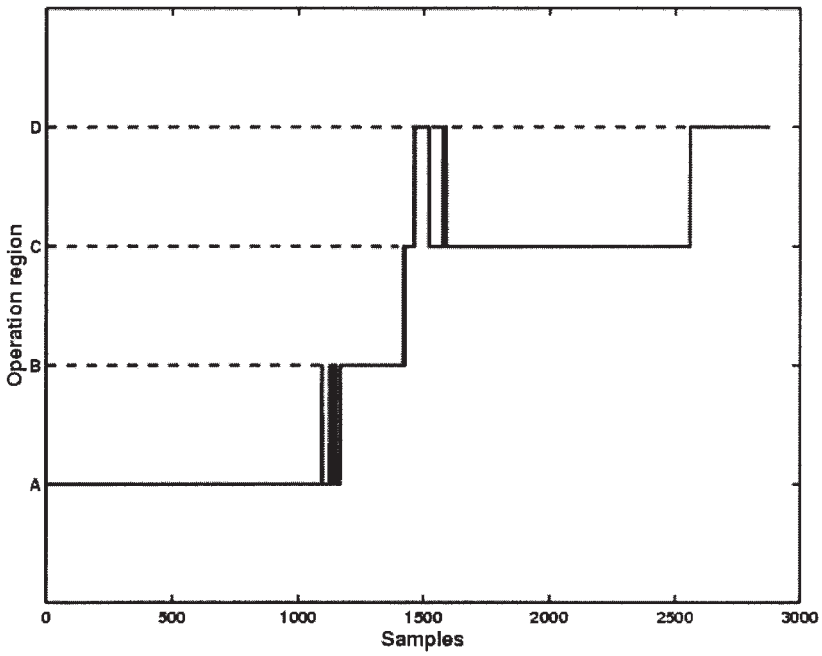


**Figure 15. Class patterns in the polyester film process data.**

for representation, whereas FDA seeks directions that are efficient for discrimination.

### *Fault diagnosis*

After the process data are classified into disjoint classes, the proposed pairwise FDA is applied to the diagnosis of faults B, C, and D. The contribution plots based on FDA fault directions for faults B, C, and D are given in Figure 18 on the lefthand side (a, c, and e, respectively). For comparison, contribution plots based on the PCA model are also given in Figure 18 on the right-hand side (b, d, and f, respectively).

*Fault B.* The contribution plot based on FDA fault direction (Figure 18a) indicates that several variables in the extrusion zone contribute to this fault. The variable plots in Figure 19 show that oscillation of several temperature loops (Variables 25 and 28) and a step change in the power of extrusion filter (Variable 32) caused this fault. However, from the contribution plot based on PCA (Figure 18b), only

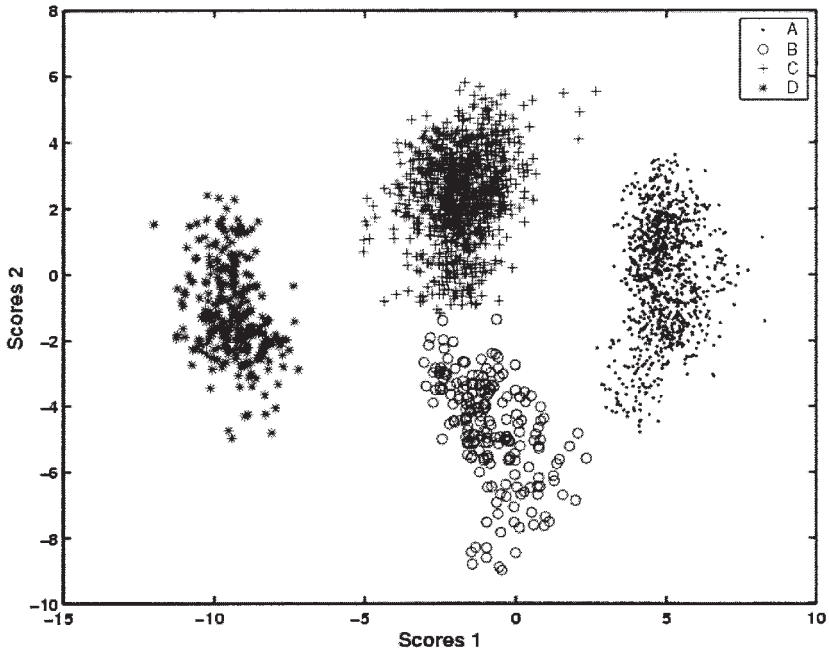


**Figure 16. Clusters in PCA score space after deleting transitional samples.**

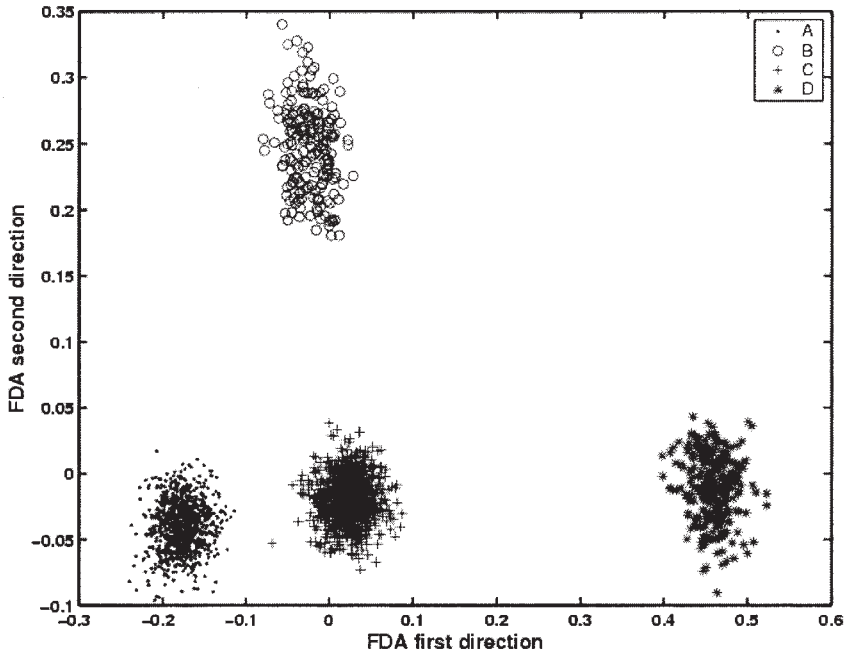


**Figure 17. Clusters in FDA Fisher space after deleting transitional samples.**

Variable 28 is identified, whereas Variables 25 and 32 are not identified.

*Fault C.* The contribution plot based on FDA fault direction (Figure 18c) reveals that a group of variables in melt pipes zone 1 caused this fault. Among them, Variables 31 and 32 are the biggest contributors. The variable plots in Figure 20 show that the offset in die flange powers (Variables 31 and 32) caused this fault. The contribution plot based on PCA (Figure 18d) also indicates that the fault occurred in the melt pipes zone 1 because a group of variables in that zone are identified. However, Variables 13 and 96 are also identified as two of the biggest contributors. Because Variable 13 is located at the extrusion zone, whereas Variable 96 is located at the tenter zone, it is unlikely that these two variables contribute to the fault occurring in the melt pipes zone 1. Besides, changes in Variable 96, as shown in Figure 20, would lead to larger SPE or $T^2$ value in Fault C than in Fault B, which is not true, as we can see from Figure 12.

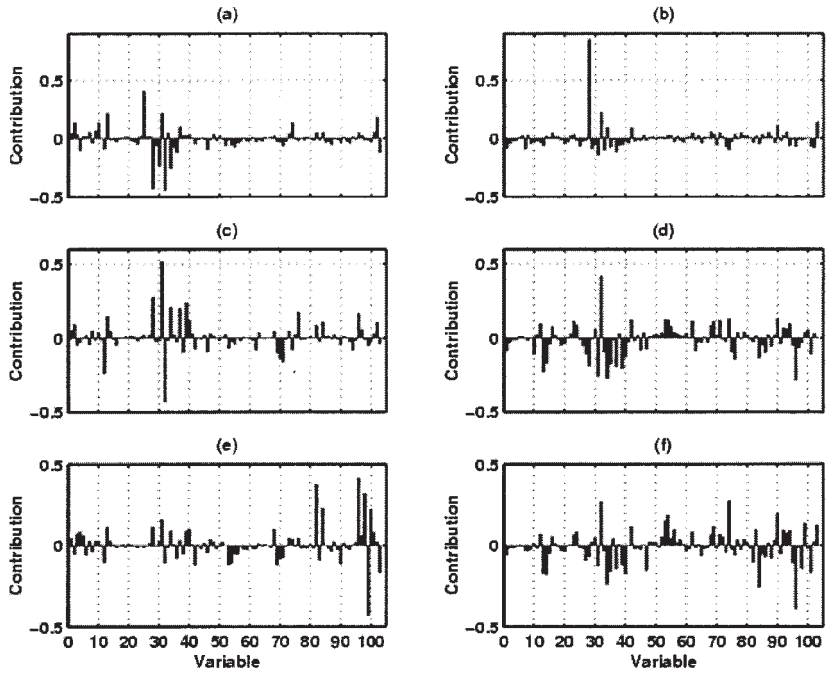


**Figure 18. Contribution plots based on FDA and PCA.**

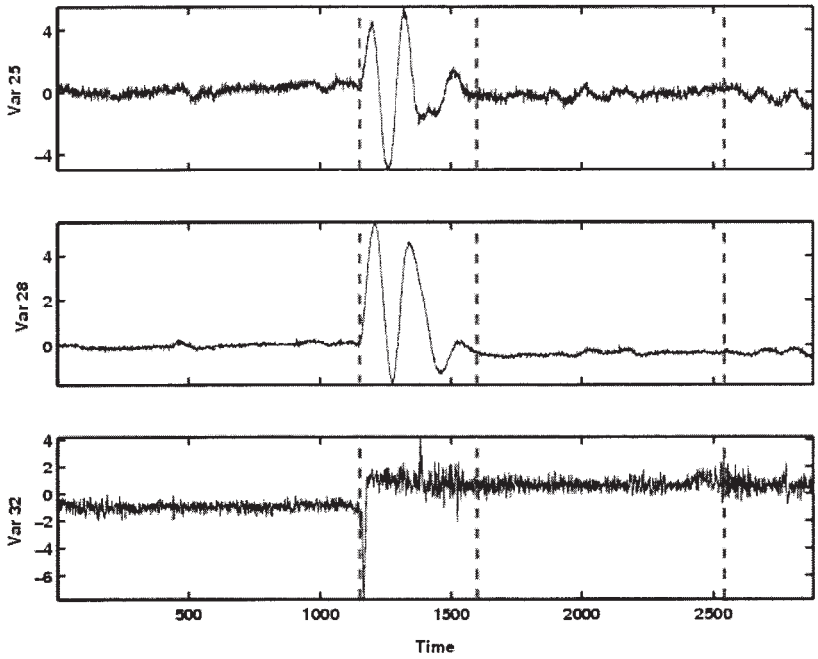


**Figure 19. Variables 25, 28, and 32 after scaling.**

*Fault D.* The contribution plot based on FDA fault direction (Figure 18e) indicates that this fault occurred in the tenter zone because several variables in that zone are identified. Process knowledge indicates that this fault is caused by the power decreases in STR reheating (Variable 82) and STR crystallizer (Variables 96 and 98) and power increase in STR cooling (Variable 99). Together these variables control the film temperature in the tenter zone. These changes affected several other variables downstream, but they do not have any impact before the die zone. The contribution plot based on PCA (Figure 18f) does not clearly indicate where this fault occurs and the contributing variables spread across the whole process, which is unlikely true. From variable plots in Figure 21, we observe sudden changes in Variables 96 and 99. We also observe that Variable 32 is not likely the root cause of this fault because there is no obvious mean or variance change during that period.

In summary, contribution plots based on FDA fault directions give better indications on which variables contribute to the faults than contribution plots based on PCA. The con-

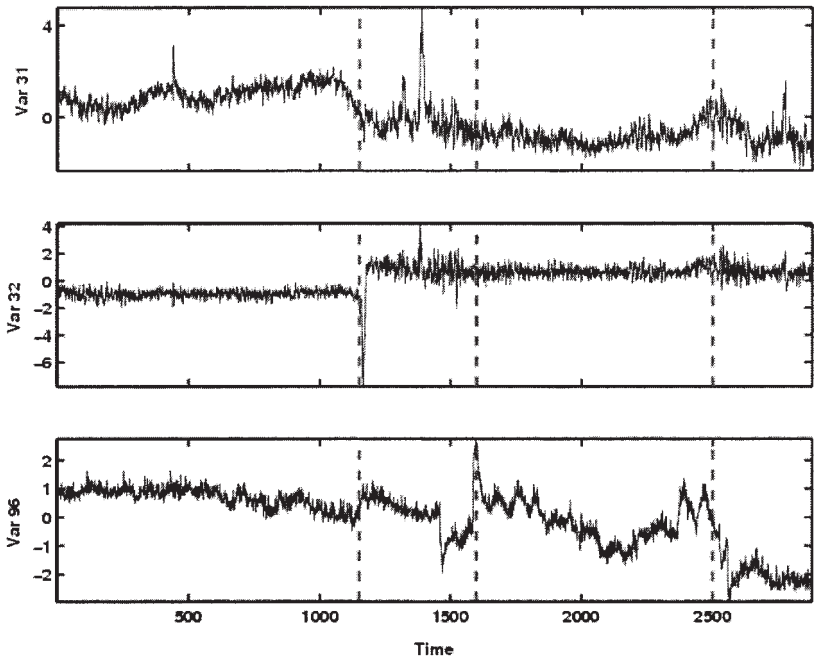


**Figure 20. Variables 31, 32, and 96 after scaling.**

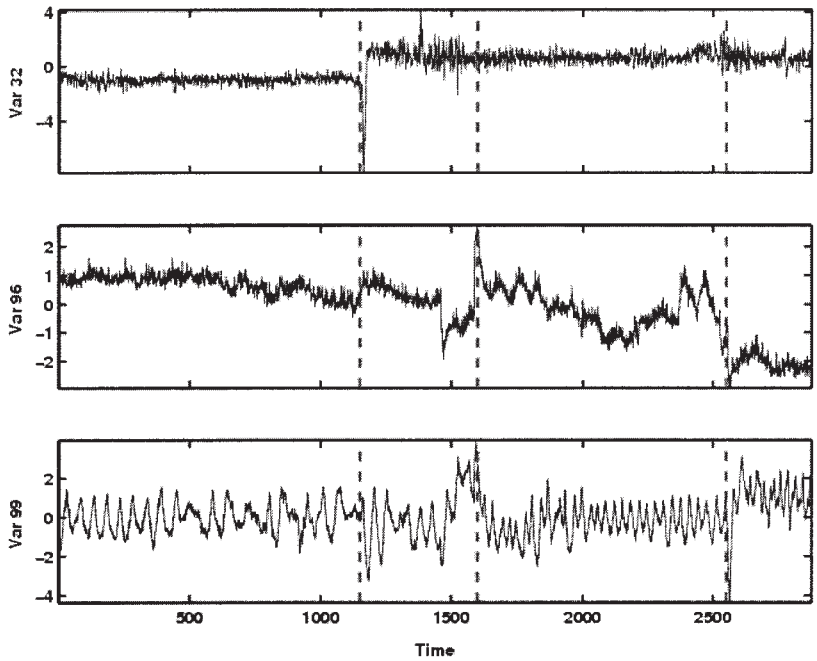


**Figure 21. Variables 32, 96, and 99 after scaling.**

tribution plots based on PCA have more difficulty in fault diagnosis at the downstream of the process because of the spread effect of the fault variables, whereas contribution plots based on FDA consistently work across the process. The superior results of FDA fault directions are attributed to the fact that FDA models the fault cluster as well as the normal data cluster, whereas PCA models only the normal data cluster.

## Conclusions

To use historical process data for process monitoring, it is imperative to isolate normal process data from a mixture of normal and abnormal historical data. The proposed three-step procedure described in this paper, consisting of preanalysis, visualization, and diagnosis, has been successfully applied to an industrial polyester film process. In the preanalysis step for fault diagnosis, the *k*-means clustering method is applied in conjunction with the PCA score chart, SPE chart, and $T^2$ chart to isolate data into different classes that correspond to different process operating regions. A clear fault visualization of high-dimensional data is obtained by applying global FDA to normal and fault data. A contribution plot based on the fault directions in pairwise FDA is proposed to enhance the ability of fault diagnosis in multivariate statistical monitoring. The proposed method is applied to a simulated quadruple-tank process, where diagnosis of the sensor fault and leakage fault has been successfully conducted. In addition, the proposed method is applied to the industrial polyester film process and provides better fault diagnosis than PCA-based contribution plots.

It is always desirable in practice to have a method that can automatically isolate historical process data into normal and fault clusters. This, however, cannot be achieved with the use of statistical methods alone. Process knowledge must be incorporated to distinguish the normal region from abnormal clusters and determine the total number of clusters. Once the normal data and the number of fault clusters are determined, the remaining steps proposed in this paper are fairly automatic. Finally, the proposed method integrates PCA, FDA, and clustering analysis to take advantage of the strength of each algorithm for a complete solution.

## Literature Cited

Benveniste, A., M. Basseville, G. Moustakides, "The Asymptotic Local Approach to Change Detection and Model Validation," *IEEE Trans. Automat. Contr.*, **32**(7), 583 (1987).

Chiang, L., E. Russell, and R. Braatz, *Fault Detection and Diagnosis in Industrial Systems*, Springer-Verlag, London (2001).

Chiang, L. H., E. L. Russell, and R. D. Braatz, "Fault Diagnosis in Chemical Processes Using Fisher Discriminant Analysis, Discriminant Partial Least Squares, and Principal Component Analysis," *Chemom. Intell. Lab. Syst.*, **50**, 243 (2000).

Conlin, A. K., E. B. Martin, and A. J. Morris, "Confidence Limits for Contribution Plots," *J. Chemom.*, **14**, 725 (2000).

Duda, R. O., P. E. Hart, and D. G. Stork, *Pattern Classification*, 2nd ed., Wiley, New York (2001).

Dunia, R., and S. J. Qin, "Subspace Approach to Multidimensional Fault Identification and Reconstruction," *AIChE J.*, **44**, 1813 (1998).

Featherstone, A. P., J. G. VanAntwerp, and R. D. Braatz, *Identification and Control of Sheet and Film Processes*, Springer-Verlag, London (2000).

Frank, P., "Fault Diagnosis in Dynamic Systems Using Analytical and Knowledge-Based Redundancy—A Survey and Some New Results," *Automatica*, **26**, 459 (1990).

Gertler, J., "Survey of Model-Based Failure Detection and Isolation in Complex Plants," *IEEE Contr. Syst. Mag.*, **12**, 3 (1988).

Hawkins, D., "The Detection of Errors in Multivariate Data Using Principal Components," *J. Am. Stat. Assoc.*, **69**, 340 (1974).

Isermann, R., "Process Fault Detection Based on Modeling and Estimation Methods—A Survey," *Automatica* **20**, 387 (1984).

Jackson, J. E., and G. Mudholkar, "Control Procedures for Residuals Associated with Principal Component Analysis," *Technometrics*, **21**, 341 (1979).

Johansson, K. H., "The Quadruple-Tank Process: A Multivariable Laboratory Process with an Adjustable Zero," *IEEE Trans. Contr. Syst. Technol.*, **8**(3), 456 (2000).

Kourti, T., and J. F. MacGregor, "Multivariate SPC Methods for Monitoring and Diagnosing of Process Performance," *Proc. of Process Syst. Eng.*, 739 (1994).
Kourti, T., and J. F. MacGregor, "Process Analysis, Monitoring and Diagnosis, Using Multivariate Projection Methods," *Chemom. Intell. Lab. Syst.*, **28**, 3 (1995).
Kourti, T., and J. F. MacGregor, "Multivariate SPC Methods for Process and Product Monitoring," *J. Qual. Technol.*, **28**, 409 (1996).
Kresta, J., J. F. MacGregor, and T. E. Marlin, "Multivariate Statistical Monitoring of Processes," *Can. J. Chem. Eng.*, **69**(1), 35 (1991).
MacGregor, J. F., "Statistical Process Control of Multivariate Processes," *Preprints Int. Federation of Automatic Control (IFAC) ADCHEM'94*, Kyoto, Japan (May 1994).
MacGregor, J. F., C. Jaeckle, C. Kiparissides, and M. Koutoudi, "Process Monitoring and Diagnosis by Multiblock PLS Methods," *AIChE J.*, **40**, 826 (1994).
Miller, P., R. Swanson, and C. Heckler, "Contribution Plots: A Missing Link in Multivariable Quality Control," *Appl. Math. Comput. Sci.*, **8**(4), 775 (1998).
Nomikos, P., "Statistical Monitoring of Batch Processes," *Preprints of Joint Statistical Meeting*, Anaheim, CA (Aug. 1997).
Qin, S. J., "Statistical Process Monitoring: Basics and Beyond," *J. Chemom.*, **17**, 480 (2003).
Qin, S. J., S. Valle-Cervantes, and M. Piovoso, "On Unifying Multi-Block Analysis with Applications to Decentralized Process Monitoring," *J Chemom.*, **15**, 715 (2001).
Raich, A., and A. Cinar, "Statistical Process Monitoring and Disturbance Diagnosis in Multivariate Continuous Processes," *AIChE J.*, **42**, 995 (1996).
Russell, E. L. and R. D. Braatz, "Fault Isolation in Industrial Processes Using Fisher Discriminant Analysis," *Foundations of Computer-Aided Process Operations*, J. F. Pekny and G. E. Blau, eds., American Institute of Chemical Engineers, New York, p. 380 (1998).
Russell, E. L., L. H. Chiang, and R. D. Braatz, *Data-Driven Techniques for Fault Detection and Diagnosis in Chemical Processes*, Springer-Verlag, London (2000).
Tong, H., and C. M. Crowe, "Detection of Gross Errors in Data Reconciliation by Principal Component Analysis," *AIChE J.*, **41**, 1712 (1995).
Westerhuis, J. A., S. Gurden, and A. Smilde, "Generalized Contribution Plots in Multivariate Statistical Process Monitoring," *Chemom. Intell. Lab. Syst.*, **51**, 95 (2000).
Wise, B., and N. Gallagher, "The Process Chemometrics Approach to Process Monitoring and Fault Detection," *J. Process Contr.*, **6**, 329 (1996).
Wold, S., K. Esbensen, and P. Geladi, "Principal Component Analysis," *Chemom. Intell. Lab. Syst*., **2**, 37 (1987).
Yoon, S., and J. MacGregor, "Fault Diagnosis with Multivariate Statistical Models, Part I: Using Steady State Fault Signatures," *J. Process Contr.*, **11**, 387 (2001).
Yue, H., and S. J. Qin, "Fault Reconstruction and Identification for Industrial Processes," *Proc. of AIChE Annual Meeting*, Miami, FL (Nov. 1998).
Yue, H., and S. J. Qin, "Reconstruction Based Fault Identification Using a Combined Index," *Ind. Eng. Chem. Res.*, **40**, 4403 (2001).

*Manuscript received Dec. 4, 2003, and revision received Jun. 10, 2004.*